

# Incipient triple point for adsorbed xenon monolayers: Pt(111) versus graphite substrates

Anthony D. Novaco\*

*Department of Physics, Lafayette College  
Easton, Pennsylvania 18042, USA*

L. W. Bruch†

*Department of Physics, University of Wisconsin–Madison  
Madison, Wisconsin 53706, USA*

Jessica Bavaresco‡

*Departamento de Física, Universidade Federal de Minas Gerais  
Caixa Postal 702, Belo Horizonte, Minas Gerais 30123-970, Brazil*

(Dated: April 27, 2015)

Simulation evidence of an incipient triple point is reported for xenon submonolayers adsorbed on the (111) surface of platinum. This is in stark contrast to the “normal” triple point found in simulations and experiments for xenon on the basal plane surface of graphite. The motions of the atoms in the surface plane are treated with standard 2D “NVE” molecular dynamics simulations using modern interactions. The simulation evidence strongly suggests an incipient triple point in the 120–150 K range for adsorption on the Pt (111) surface while the adsorption on graphite shows a normal triple point at about 100 K.

PACS numbers: 68.43.-h, 68.35.Md, 68.35.Rh, 64.70.Rh

Keywords: adsorption, monolayer, xenon, Pt (111), graphite, molecular dynamics

The adsorption of xenon on the (111) surface of platinum (Xe/Pt) is one of the more interesting cases of physical adsorption. The potential energy surface is very strongly corrugated and a wide variety of monolayer structures occur.<sup>1</sup> The binding to the surface is relatively large, so that the vapor pressure coexisting with the monolayer remains small enough at temperatures approaching monolayer melting that experimental probes such as low energy electron diffraction and helium atom scattering remain viable. Thus, direct measurements of monolayer dynamics near melting, which are very scarce in the family of nominally two-dimensional systems, may be feasible in this case.

The corrugation for Xe/Pt is much larger than it is for xenon on the basal plane of graphite (Xe/Gr).<sup>2–5</sup> The Xe/Pt minimum barrier to translation from one adsorption site to the next is roughly 275 K, whereas the minimum in the effective interaction between two Xe atoms is about 238 K (for Xe/Gr, the barrier is about 50 K.). This should produce strong competition between atom-atom forces and atom-substrate forces. However, there is a report<sup>6</sup> that the Xe/Pt triple point temperature is  $98 \pm 2$  K, essentially equal to that of Xe/Gr,<sup>1,5</sup> a surface with a smaller corrugation<sup>3,4</sup> by a factor of about 5 or 6. While it is expected that thermal excitations will somewhat smooth the effects of substrate corrugation,<sup>3</sup> and this indeed is the case with Xe/Gr,<sup>4,5</sup> results of preliminary molecular-dynamics calculations<sup>7</sup> for Xe/Pt indicate there is insufficient smoothing to explain such similar triple point temperatures. The results of those preliminary calculations suggest there should be a measurable effect upon the triple point of Xe/Pt as a result of this

corrugation. Dilemma: Why should a system with such strong corrugation behave so like a system with rather weak corrugation?<sup>5</sup>

The strong corrugation of the Xe/Pt system and the fact that the monolayer apparently melts from the commensurate solid phase<sup>6</sup> suggests an interesting possibility: the existence of an incipient triple point. This can occur if the substrate corrugation is strong enough to sufficiently lower the free energy of the solid phase so as to maintain a direct transition from the solid phase into the gas phase, bypassing the liquid phase altogether.<sup>8,9</sup> With Xe/Pt, we not only have strong corrugation, but also a dilated Xe lattice which weakens the effects of the attractive region of the Xe-Xe interaction. This dilation is due to the  $\sqrt{3} \times \sqrt{3}$ -R30° phase ( $\sqrt{3}$  phase) having a lattice spacing<sup>10</sup> of 4.80 Å, which is significantly larger than the “natural” lattice spacing of the Xe, that being in the 4.38–4.55 Å range.<sup>5</sup> This implies Xe atoms, when they are located on the  $\sqrt{3}$  adsorption sites, tend to be kept away from the hard-core region of their mutual interaction and found in the weaker region of their attractive well. Therefore, there exists the possibility that this system will, at high temperatures, act much like a lattice gas on a triangular lattice (here, exhibiting repulsive nearest neighbors and attractive next-nearest neighbor interactions). This is an interesting possibility since transitions in similar systems have been examined theoretically,<sup>11</sup> including renormalization group calculations.<sup>12,13</sup> The results reported in this communication are part of a much larger study<sup>14</sup> of the structure and thermodynamics of Xe/Pt. The results reported here for Xe/Gr build upon the analysis reported in Ref. 5.

The simulation model for Xe/Pt is the Xe/Gr model<sup>5</sup> adapted to Xe/Pt with new parameters for the substrate-mediated interaction and a much larger potential energy corrugation.<sup>3,15</sup> Validation of the resulting model for Xe/Pt is mainly based on the analysis<sup>15</sup> of the stability and dynamics of a compressed triangular lattice of Xe/Pt with nearest neighbor spacing 4.33 Å. The Barker-Rettner (BR) model<sup>2</sup> is used for the 3D potential energy surface of Xe/Pt as in Ref. 3. In this work, the BR interaction is simplified by first using a 2D version of the 3D Steele expansion,<sup>16</sup> and then truncating the sum in reciprocal space (consistent with the substrate's 6-fold symmetry). Thus

$$U(\mathbf{r}) = U_{(1,0)} \sum_{\mathbf{G}} \exp(i\mathbf{G} \cdot \mathbf{r}), \quad (1)$$

where  $U$  is the potential energy of the Xe atom in the field of the substrate,  $\mathbf{r}$  is the displacement vector of the atom parallel to the surface, and  $\mathbf{G}$  is a member of the set of the six shortest reciprocal lattice vectors defined for the surface lattice.

The simulations carried out are standard NVE molecular dynamics simulations in 2D (here NVE being the 2D version: Number-Area-Energy). The implementation of the basic simulation is exactly as per Refs. 4 and 5, using essentially the same set of parameters. As in those works, we examined both constrained geometries (a single phase filling the simulations box) and unconstrained geometries (an isolated patch surrounded by vapor). The density of the  $\sqrt{3}$  structure is denoted by  $\rho_p$  for Xe/Pt and by  $\rho_g$  for Xe/Gr. Simulations for the unconstrained geometries are for average densities  $\rho$  that are roughly half that of the corresponding  $\sqrt{3}$  phase. In addition to the thermodynamic quantities calculated in Ref. 5 (such as the hexatic order parameter  $\psi_6$ ), calculations are carried out for the specific heat at constant area  $c_a$  and a second order parameter: the “Net-Domain-Phase” (NDP) order parameter. The set of case studies reported here are detailed in Table I.

Calculations for  $c_a$  use the fluctuations in the kinetic energy of the system.<sup>17</sup> As a consequence of this approach, there are some problems in evaluating  $c_a$  when the drift in the energy is too large over the averaging time interval, as this can result in negative values for  $c_a$ . Nevertheless, most of the calculations result in values that are consistent with the slope of the total energy versus temperature data.<sup>18</sup> However, the latter approach also generates some values which are negative (resulting from statistical uncertainty in the thermodynamic quantities). Negative values for  $c_a$  (as well as some very large positive values) are not included in the plots.

The NDP order parameter is important in determining and understanding the nature of the order-disorder transition in Xe/Pt. It is defined by:

$$\psi_0 = \frac{1}{N} \sum_{i=1}^N \exp(i\boldsymbol{\tau}_{(1,0)} \cdot \mathbf{r}_i), \quad (2)$$

TABLE I. Parameters that define the various case studies discussed in this paper. All energy values are in kelvin.

Case Study	Substrate	Projection	Size	$U_{(1,0)}$
U36-64K <sup>a</sup>	Pt (111)	U36	64K	-35.6
U36H-20K <sup>b</sup>	Pt (111)	U36H	20K	-35.6
U15H-20K <sup>b</sup>	Pt (111)	U15H	20K	-15.0
U6H-78K <sup>c</sup>	Graphite	U6H	78K	-6.0

<sup>a</sup> Constrained geometry with 65536 adatoms.

<sup>b</sup> Unconstrained geometry with 20064 adatoms.

<sup>c</sup> Unconstrained geometry with 78000 adatoms.

where  $N$  is the number of Xe atoms and  $\boldsymbol{\tau}_{(1,0)}$  is a primitive reciprocal lattice vector for the Xe  $\sqrt{3}$  structure. This order parameter is, of course, nothing more than the basic structure factor evaluated at  $\boldsymbol{\tau}_{(1,0)}$  and is a sensitive test of the lattice gas ordering in the  $\sqrt{3}$  commensurate lattice. If all the atoms are placed on the ideal lattice sites of a  $\sqrt{3}$  phase single domain, this order parameter takes on a value in the set: (1.0,  $e^{i2\pi/3}$ , and  $e^{-i2\pi/3}$ ); the particular value depends upon which of the three possible site types (sub-lattices) is occupied. The NDP order parameter is zero if each adsorption site type is populated with equal probability, even if that phase is not one of true disorder, e.g. the hexagonal incommensurate phase (HIC) or the striped incommensurate phase (SI).

Simulations of constrained geometries are used to determine the stable low temperature phase for the classical system and in the interpretation of the high temperature behavior for a parallel set of unconstrained geometries. The constrained geometries are also used to test the sensitivity of the simulations to system size and to follow the system in a simpler context (having only one phase present at any given temperature). However, the transition temperature for the constrained geometries is quite high, and not relevant to the experimental conditions. In fact, it would be expected that layer promotion would become quite important well before the transition would be reached for these constrained geometries. Simulations of the unconstrained geometries are used to examine both the thermal behavior and the structural properties of the submonolayer patch. These configurations generally show 2-phase coexistence of a 2D gas and a 2D dense phase (most cases follow the 2D sublimation curve).

The 2D projection (at very low temperatures) of the BR model for Xe/Pt gives<sup>19</sup>  $-36 \text{ K} \leq U_{(1,0)} \leq -34 \text{ K}$ . This is obtained by assigning the BR energy barrier to the corrugation given by Eq. (1). For Xe/Pt, this corrugation produces a  $\sqrt{3}$  structure for the ground state. However, simulations carried out for smaller corrugations test both the stability of the  $\sqrt{3}$  ground state to variations in the corrugation and address the issue of the effective corrugation being dependent on temperature due to the thermal motion of the Xe in the direction normal to the surface.<sup>3,14,20</sup> Thermal vibration of the adatom normal to the surface causes the effective corrugation to decrease as the temperatures increases.<sup>3,14</sup> Although we have exam-

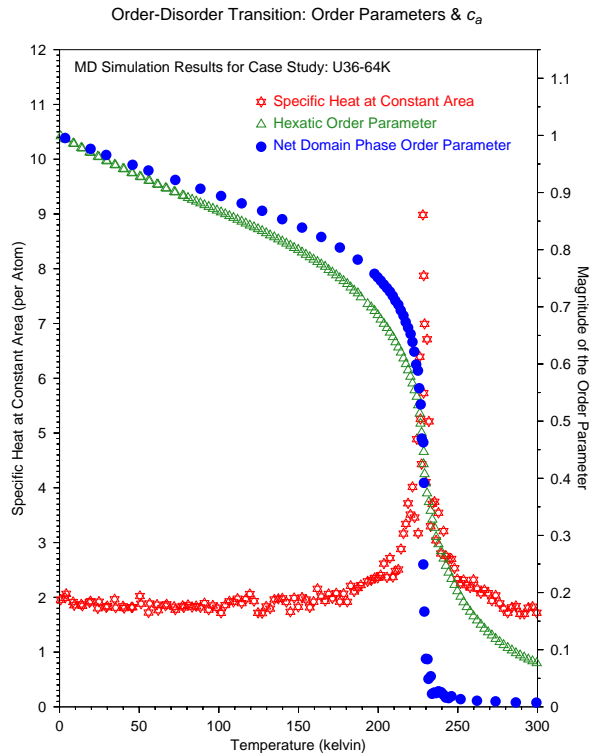


FIG. 1. (Color online) The hexatic order parameter, the NDP order parameter, and the specific heat for case study U36-64K of Xe/Pt, showing the alignment of the peak in the specific heat with the sharp drop in value of  $\psi_0$ . The density is  $\rho_p$ .

ined a number of corrugation values, we report only those listed in Table I. While the HIC structure is the ground state for the smaller corrugation, both high and low corrugation cases for the unconstrained geometries exhibit a stable  $\sqrt{3}$  structure below melting. This behavior is independent of the different initialization structures ( $\sqrt{3}$  or HIC) generated for the system. However, for the U15H case the transition from HIC to  $\sqrt{3}$  occurs just below melting.

Examination of the heating data for case study U36-64K shows a distinct transition from an ordered to a disordered state at about 230 K. Figure 1 shows the specific heat and the magnitudes of the order parameters  $\psi_0$  and  $\psi_6$ . The specific heat shows clear signs of a transition, with a moderate to large increase in its value and a classic  $\lambda$  shape. As the temperature is increased,  $\psi_0$  clearly shows a sharp drop in its value while  $\psi_6$  displays a more gradual decrease in the orientational order of the system. The specific heat peak is aligned very nicely with the sharp decrease in  $\psi_0$  and suggests that  $\psi_0$  is a good measure of this order-disorder transition. Furthermore, the specific heat is more suggestive of a classic continuous transition than of the traditional discontinuous transition of a triple point constrained by a fixed area (which would have a trapezoidal profile). It is relevant here to be mindful that the natural spacing of the Xe atoms is smaller than the spacing in the  $\sqrt{3}$  structure. Thus the usual situation of a triple point being associated with an

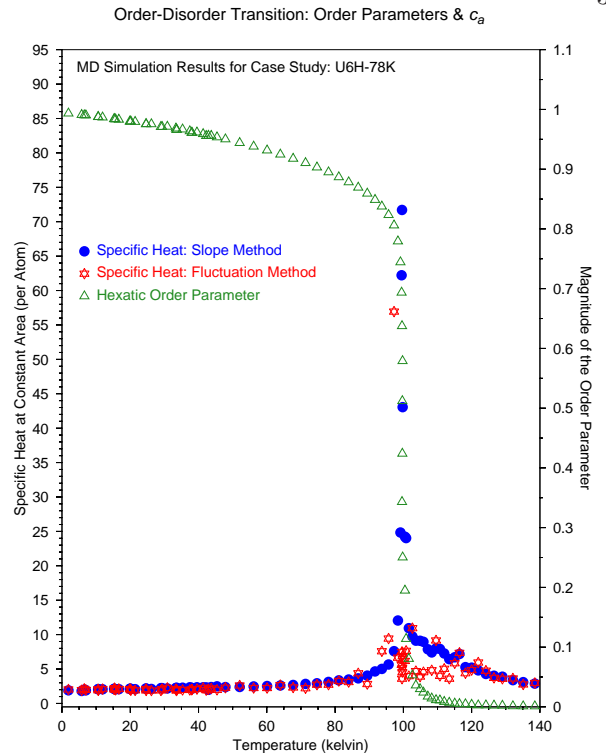


FIG. 2. (Color online) The hexatic order parameter and the specific heat for case study U6H-78K of Xe/Gr, comparing methods for the calculation of the specific heat. The average density is about  $\rho_g/2$ .

increase in area is not relevant and the structure seems to be dominated by the corrugation of the substrate even at the (incipient) triple point.

The results for Xe/Pt are different from those obtained for Xe/Gr, where there is clear evidence, within statistical uncertainty, of a vertical rise in the energy at a fixed temperature.<sup>5</sup> This results in a specific heat that has a sharp (almost vertical) rise in the specific heat and a much smaller precursor to this sharp rise as seen in Fig. 2, where the hexatic order parameter shows a sharp drop in its value. This drop is well aligned with the vertical rise in the total energy, implying that  $\psi_6$  is a good measure of the order-disorder in the Xe/Gr system.<sup>5</sup>

All these behaviors are consistent with structure factor plots of each system showing a clear loss of order as the system moves through the corresponding transition.<sup>5,14</sup> However, for Xe/Pt, there is no clear indication of a self-bound liquid state in the spatial plots of the system as there is<sup>4,5</sup> for Xe/Gr. Figure 3 shows a distinct liquid-gas interface for Xe/Gr just above its triple point, but no hint of such an interface for Xe/Pt just above its order-disorder transition. In both cases, these plots are for initially hexagonal patches centered in the simulation cell. For Xe/Pt, there is no evidence of a discontinuous transition; rather there is evidence of a likely continuous one. For the unconstrained geometries, there tends to be more scatter in the data, and both order parameters drop more gradually to zero (as compared to the constrained

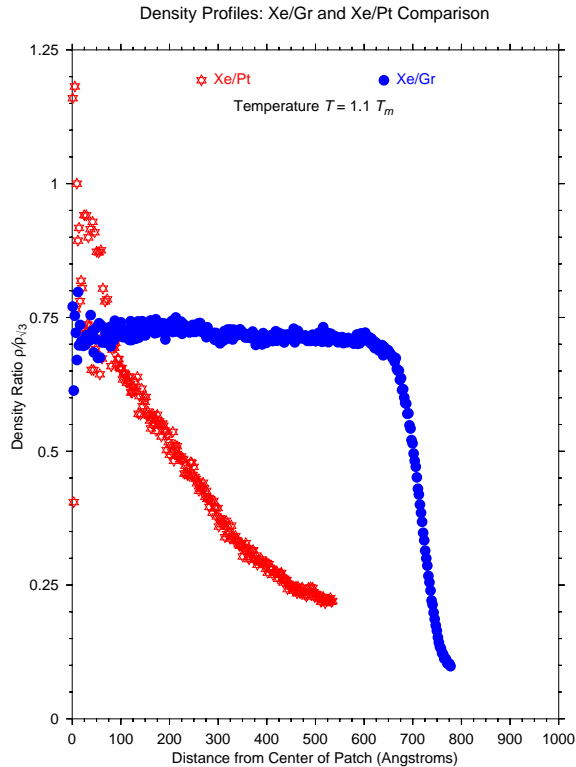


FIG. 3. (Color online) Comparison of the density profiles for patches of Xe/Gr (case study U6H-78K;  $T_m \simeq 100$  K;  $\rho \simeq \frac{1}{2}\rho_g$ ) and Xe/Pt (case study U36H-20K;  $T_m \simeq 150$  K;  $\rho \simeq \frac{1}{2}\rho_p$ ) just above the melting (order-disorder) transition.

geometries). For U36H-20K, the transition temperature is  $\simeq 150$  K, significantly lower than that for U36-64K, but still significantly higher than the experimental value<sup>6</sup> of  $\simeq 100$  K.

At temperatures near the transition temperature, the corrugation is smoothed by the thermal motion perpendicular to the surface (lateral motion smoothing is part of the MD simulation). Preliminary estimates of smoothing<sup>14</sup> at these high temperatures result in  $|U_{(1,0)}|$  values in the 20–25 K range, corrugations which still produce order-disorder temperatures higher than the experimental value. Question: How large must the smoothing be to bring the simulation results closer to the experimental temperature? In Fig. 4, the effects of extreme smoothing are shown using a  $U_{(1,0)}$  of  $-15$  K. The transition temperature is about 120 K, significantly lower than that of the U36H-20K case study.

The  $\psi_0$  order parameter appears to be a better measure than  $\psi_6$  for the order-disorder associated with the transition from solid to fluid in the Xe/Pt system. The drop in the order parameter with increasing temperature near the transition is steeper and more complete for  $\psi_0$  than it is for  $\psi_6$ . Furthermore,  $\psi_0$  is more sensitive than is  $\psi_6$  to system size,<sup>14</sup> and this is what would be expected if  $\psi_0$  is the more thermodynamically relevant order parameter. This is in stark contrast to the results for Xe/Gr,<sup>5</sup> where  $\psi_6$  is a very good measure of the order-disorder near the triple point of that system as shown in Fig. 2.

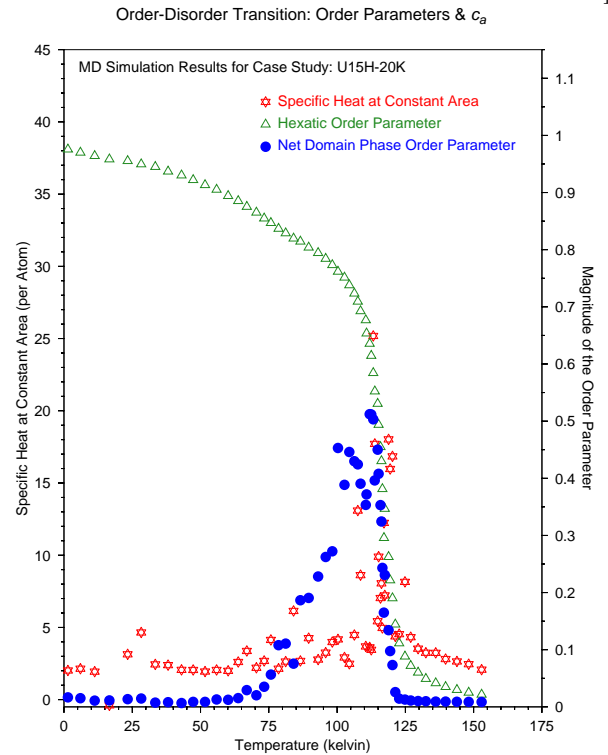


FIG. 4. (Color online) The hexatic order parameter, the NDP order parameter, and the specific heat for case study U15H-20K of Xe/Pt, showing the alignment of the peak in the specific heat with the sharp drop in value of  $\psi_0$ . The average density is about  $\rho_p/2$ .

The melting of Xe/Pt is clearly of a different nature than the true triple point melting of Xe/Gr. This can be seen by the differences in the specific heats, order parameters, and structural orderings of the two systems. These calculations and other observations of the solid<sup>20,21</sup> above 100 K make it likely the phenomenon at 98 K in Ref. 6 is not triple point melting. These simulations suggest that a Xe/Pt triple point at  $\simeq 100$  K is inconsistent with the observation of a  $\sqrt{3}$  phase at 60 K. The case of Xe/Pt has all the earmarks of an incipient triple point as described in Ref. 8, having a specific heat that looks much like that of a lattice gas transition as described in Ref. 13. Since there are finite-size effects (as there are in any simulation), it is not possible to rule out a normal triple point and a normal critical point separated by a small temperature gap. However, such effects would also bedevil the experimental systems. Studies on larger systems having longer run times would be welcome, as well as a better understanding of the thermal smoothing of the corrugation. More thorough experimental studies of the dense monolayer at 100–125 K (such as measurements of diffusive motions) might be decisive in establishing the way in which the monolayer disorders.

## ACKNOWLEDGMENTS

We would like to acknowledge and thank C. Chen and S. Kapita for the work they did on the preliminary studies that preceded this work. We also thank

Lafayette College for its generous support and the Computer Science Department of Lafayette College for use of their research computer cluster. Jessica Bavaresco's exchange visit to Lafayette College during the 2012 calendar year was sponsored by the Brazilian government agency CAPES as part of the Science Without Borders program.

- 
- \* E-mail: novacoad@lafayette.edu  
 † E-mail: lwbruch@wisc.edu  
 ‡ E-mail: jbavaresco@ufmg.br
- <sup>1</sup> L. W. Bruch, R. D. Diehl, and J. A. Venables, *Rev. Mod. Phys.* **79**, 1381 (2007).
  - <sup>2</sup> J. A. Barker and C. T. Rettner, *J. Chem. Phys.* **97**, 5844 (1992).  
 Erratum: J. A. Barker and C. T. Rettner, *J. Chem. Phys.* **101**, 9202 (1994).
  - <sup>3</sup> L. W. Bruch and A. D. Novaco, *Phys. Rev. B* **61**, 5786 (2000).
  - <sup>4</sup> L. W. Bruch and A. D. Novaco, *Phys. Rev. B* **77**, 125435 (2008).
  - <sup>5</sup> A. D. Novaco and L. W. Bruch, *Phys. Rev. B* **89**, 125431 (2014).
  - <sup>6</sup> B. Poelsema, L. Verheij, and G. Comsa, *Surf. Sci.* **152–153, Part 2**, 851 (1985).
  - <sup>7</sup> A. D. Novaco, C. Chen, and S. Kapita (unpublished).
  - <sup>8</sup> K. J. Niskanen, *Phys. Rev. B* **33**, 1830 (1986).
  - <sup>9</sup> K. J. Niskanen and R. B. Griffiths, *Phys. Rev. B* **32**, 5858 (1985).
  - <sup>10</sup> K. Kern, R. David, P. Zeppenfeld, and G. Comsa, *Surf. Sci.* **195**, 353 (1988).
  - <sup>11</sup> M. Schick and R. L. Siddon, *Phys. Rev. A* **8**, 339 (1973).
  - <sup>12</sup> M. Schick, J. S. Walker, and M. Wortis, *Phys. Rev. B* **16**, 2205 (1977).
  - <sup>13</sup> M. Schick, J. S. Walker, and M. Wortis, *J. Phys. (Paris)* **C-4**, 121 (1977).
  - <sup>14</sup> A. D. Novaco and J. Bavaresco (unpublished).
  - <sup>15</sup> L. W. Bruch, A. P. Graham, and J. P. Toennies, *J. Chem. Phys.* **112**, 3314 (2000).
  - <sup>16</sup> W. A. Steele, in *The Interaction Of Gases With Solid Surfaces* (Pergamon Press, Oxford, New York, 1974), vol. 3 of *The International Encyclopedia Of Physical Chemistry And Chemical Physics. Topic 14: Properties Of Interfaces* (Pergamon Press, Oxford, New York, 1974).
  - <sup>17</sup> J. L. Lebowitz, J. K. Percus, and L. Verlet, *Phys. Rev* **153**, 250 (1967).
  - <sup>18</sup> The slope is determined by a numerical derivative of the total energy, using second order fits to sequential sets of data triplets.
  - <sup>19</sup> The exact value depends upon the calculational details. These include: how to assign the corrugation to a single Fourier amplitude, what approximations are made for the variation of the Fourier amplitudes in the direction normal to the surface, and how the zero-point energy associated with that direction is treated.
  - <sup>20</sup> T. Seyller, M. Caragiu, R. D. Diehl, P. Kaukasoina, and M. Lindroos, *Phys. Rev. B* **60**, 11084 (1999).
  - <sup>21</sup> D. J. Ward, D. phil., University of Cambridge, England (2013), and J. E. Ellis (private communication).